The Effects of the Coupled Slotline Mode and Air-Bridges on CPW and NLC Waveguide Discontinuities

Chung-Yi Lee, *Student Member, IEEE,* Yaozhong Liu, *Student Member, IEEE,* and Tatsuo Itoh, *Fellow, IEEE*

Abstract— **The extended spectral domain analysis is applied to analyze symmetrical and asymmetrical coplanar and nonleaky coplanar waveguide discontinuities. The three-dimensional dyadic Green's function is derived first to calculate the contributions of horizontal (vertical) magnetic (electrical) currents. No air-bridges are needed if the discontinuity is symmetrical. It is shown that the coupled slotline (CSL) mode excited by asymmetrical discontinuities drastically affects the CPW circuit performance. The effect of air-bridges used to suppress the unwanted CSL mode is studied. Experimental data agree very well with numerical results for CPW discontinuities. In addition, the discontinuities of a novel conductor-backed CPW structure, the nonleaky coplanar (NLC) waveguide, are also investigated. From experiment, it is found that the SMA-to-NLC transition causes power leakage. Except for the small leakage, theoretical and experimental results agree well.**

I. Introduction

THE COPLANAR waveguide (CPW) is extensively used in monolithic microwave integrated circuits (MMIC's). It provides some better electrical and mechanical properties than microstrip circuits. Nevertheless, there are two dominant modes, CPW and coupled slotline (CSL) modes, that exist in CPW's which consist of three conductors. This wave-guiding characteristic causes some problems in the application of CPW's if a single-mode operation is required. In real circuit layouts, both symmetrical and asymmetrical discontinuities exist commonly. For symmetrical circuits, no air-bridge are needed, as discussed in [1]. However, the CPW-to-CSL mode conversion or vice versa would unavoidably happen if there are asymmetries in the structure. Then the air-bridge is usually used to suppress the unwanted CSL mode and to enforce the single CPW mode operation on the circuit.

Some literature had discussed the electrical performance of symmetrical and asymmetrical CPW circuits with or without air-bridges. Experimental investigations of various air-bridge configurations used for MMIC's in CPW techniques were presented in [2]. The effect of the air-bridge height on microstrip circuits was modeled by using the hybrid spectral domain and quasi-TEM techniques [3]. A series of studies of various CPW discontinuities with and without air-bridges using the hybrid analysis technique was conducted by N. I. Dib *et al.* [4]–[6]. In their analysis, the equivalent circuit of CPW discontinuities without air-bridges was formulated first using the space domain integral equation. Then, the circuit was modified by incorporating the parasitic inductance and capacitance of the air-bridge, which were evaluated using a simple quasi-static model. Various full-wave techniques had also been used extensively to analyze different CPW configurations with air-bridges, e.g., the frequency-domain TLM method [7], the complex image technique [8], the extended spectral domain analysis [9], and the FDTD method [10]. But in these references, the effect of the CSL mode on asymmetrical CPW discontinuities without air-bridges is not investigated completely, and there are insufficient parametric data for the air-bridge design to effectively suppress the CSL mode. Hence, the objectives of this paper are to study the danger of the CSL mode and to provide more design information for CPW one-port discontinuities.

The conductor-backed coplanar waveguide (CBCPW) provides superior mechanical strength and the heat sinking ability than conventional CPW's. The inherent characteristic of power leakage in terms of the parallel-plate wave, however, makes the CBCPW an impractical wave-guiding structure [11]. The leakage causes unwanted crosstalk and package effects. Therefore, how to suppress the power leakage is an important step to make the CBCPW practical and useful. Recently, some efforts had been done to study the origin and leakage control of uniform CBCPW's [12]–[14]. The nonleaky coplanar (NLC) waveguide proposed in [12] has the benefits of easy fabrication, high tolerance to the change of dimensions, and high mechanical strength. The one with an additional bottom layer is especially suitable for MMIC's because it is easy to add air-bridges if necessary. In addition to uniform lines, the effects of discontinuities on these nonleaky structures should be evaluated. This paper is also devoted to studying symmetrical and asymmetrical one-port discontinuities of the NLC waveguide. In our analysis, the air-bridge is added to the asymmetrical structure to suppress the CSL mode on NLC structures.

The 3-D spectral domain analysis (SDA) is employed to analyze these uniplanar structures. By the formulation of the exact Green's function, all physical effects are taken into account. This extended method was first proposed to analyze microstrip structures with a bond wire by Becks and Wolff [15]. The method had also been applied successfully to simulate microstrip circuits with passive and active lumped

Manuscript received February 15, 1995; revised July 7, 1995. This work was supported by the TRW MICRO.

The authors are with the Department of Electrical Engineering, University of California, Los Angeles, Los Angeles, CA 90095 USA.

IEEE Log Number 9415484.

elements [16], microstrip structures with metallization thickness [17], and a shorting pin in multilayered circuits [18]. In Section II, the key features of applying the extended SDA are described. Since the input line is terminated with the SMA connector, the CPW mode is the only one that can be launched and measured in our test setup. By assuming that the connector is a short circuit for the CSL mode, the relationship between the simulated and measured scattering parameters is derived. The good agreement between the numerical result and the measurement is shown in Section III. The effects of the CSL mode and air-bridges on the circuit performance are discussed. Extensive experimental investigations and discussions of power leakage caused by the SMA-to-NLC transition are also demonstrated. Finally, brief conclusions are given in Section IV.

II. Theoretical Formulation

A. Spectral Domain Analysis

Fig. 1 depicts the geometry of a NLC waveguide one-port discontinuity, which can be symmetrical or asymmetrical. It can be changed into the conventional CPW by letting $\varepsilon_{r2} = 1$ and h_2 approach infinity. The substrate and conductors are assumed to be lossless and infinite in the xy-plane. Since there are detailed derivation processes available in [15], only key features of the 3-D SDA are described here. The first step of the SDA is the derivation of the spectral domain dyadic Green's function. Both horizontal (x- or y-directed) and vertical (z-directed) Hertzian dipoles and electromagnetic field components are utilized to formulate the entire 3-D dyadic Green's function of Fig. 1. The derivation processes for the horizontal dipoles are the same as the conventional SDA except that vertical field components are calculated now. An extension to vertically directed current elements is introduced to incorporate the existence of the air-bridge. Since the air-bridge is very small compared with the guided wavelength, it is assumed that there is only linear (1-D) current flowing on it. Both transverse and longitudinal slot fields on the planar CPW are taken into account. After all boundary conditions are matched, the 3-D spectral domain Green's function with the air-bridge is as shown in (1) at the bottom of the page, where α and β are two spectral variables defined in the x and y direction. z and z_s are vertical observation and source points, respectively.

The next step is to represent slot fields on the CPW and currents on the air-bridge using appropriate basis functions with unknown coefficients. In this paper, piecewise-linear (rooftop) functions are used to express x- and y-directed slot fields. The air-bridge is modeled as two rectangular posts connected by a conductor strip with negligible thickness. The

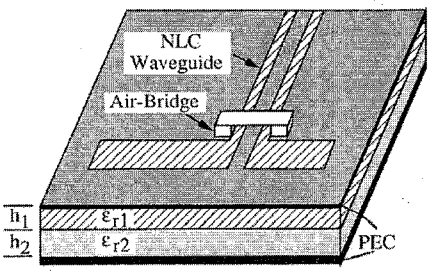

(a)

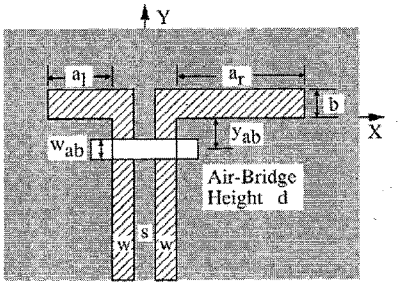

(b)

Fig. 1. The nonleaky coplanar (NLC) waveguide discontinuity. (a) 3-D plot. (b) Top view.

horizontal strip current is expanded by the x-directed rooftop function. The vertical post current is described by a surface current density using the pulse function. Generally, the z-dependence can be integrated numerically. Because of the choice of the pulse function, the vertical dependence can be integrated analytically. After some manipulations, (1) is transformed into decaying functions of two spectral variables α and β only.

With the basis functions appropriately set up, the analysis procedure is divided into two parts: eigenvalue analysis and scattering parameters calculation [19]. The first part is used to provide the uniform line characteristics which will be utilized in the second part for waves on the input port. To compute scattering parameters in the second part, the Galerkin procedure is applied to generate a set of linear equations

$$\begin{bmatrix} \boldsymbol{Y}_{xx}^{11} & \boldsymbol{Y}_{xy}^{11} & \boldsymbol{T}_{xx}^{12} & \boldsymbol{T}_{xz}^{13} \\ \boldsymbol{Y}_{yx}^{11} & \boldsymbol{Y}_{yy}^{11} & \boldsymbol{T}_{yx}^{12} & \boldsymbol{T}_{yz}^{13} \\ \boldsymbol{T}_{xx}^{21} & \boldsymbol{T}_{xy}^{21} & \boldsymbol{Z}_{xx}^{22} & \boldsymbol{Z}_{xz}^{23} \\ \boldsymbol{T}_{zx}^{31} & \boldsymbol{T}_{zy}^{31} & \boldsymbol{Z}_{zx}^{32} & \boldsymbol{Z}_{zz}^{33} \end{bmatrix} \begin{bmatrix} \boldsymbol{E}_x \\ \boldsymbol{E}_y \\ \boldsymbol{J}_x \\ \boldsymbol{J}_z \end{bmatrix} = \begin{bmatrix} \boldsymbol{J}_x \\ \boldsymbol{J}_y \\ \boldsymbol{V}_x \\ \boldsymbol{V}_z \end{bmatrix}. \quad (2)$$

In (2), each term in the 4×4 matrix on the left-hand side and the column matrix on the right-hand side is a submatrix which represents a set of self or mutual interactions between expansion and testing functions. The field/current distributions and reflection coefficients for different modes can be obtained by taking the inverse matrix operation of (2). The discontinuity

$$\begin{bmatrix} \tilde{J}_x(\alpha,\beta,0) \\ \tilde{J}_y(\alpha,\beta,0) \\ \tilde{E}_x(\alpha,\beta,d) \\ \tilde{E}_z(\alpha,\beta,z) \end{bmatrix} = \begin{bmatrix} \tilde{G}_{xx}^{11}(\alpha,\beta,0) & \tilde{G}_{xy}^{11}(\alpha,\beta,0) & \tilde{G}_{xx}^{12}(\alpha,\beta,d) & \tilde{G}_{xz}^{13}(\alpha,\beta,z_s) \\ \tilde{G}_{yx}^{11}(\alpha,\beta,0) & \tilde{G}_{yy}^{11}(\alpha,\beta,0) & \tilde{G}_{yx}^{12}(\alpha,\beta,d) & \tilde{G}_{yz}^{13}(\alpha,\beta,z_s) \\ \tilde{G}_{xx}^{21}(\alpha,\beta,0) & \tilde{G}_{xy}^{21}(\alpha,\beta,0) & \tilde{G}_{xx}^{22}(\alpha,\beta,d) & \tilde{G}_{xz}^{23}(\alpha,\beta,z_s) \\ \tilde{G}_{zx}^{31}(\alpha,\beta,z) & \tilde{G}_{zy}^{31}(\alpha,\beta,z) & \tilde{G}_{zx}^{32}(\alpha,\beta,z) & \tilde{G}_{zz}^{33}(\alpha,\beta,z,z_s) \end{bmatrix} \cdot \begin{bmatrix} \tilde{E}_x(\alpha,\beta,0) \\ \tilde{E}_y(\alpha,\beta,0) \\ \tilde{J}_x(\alpha,\beta,d) \\ \tilde{J}_z(\alpha,\beta,z) \end{bmatrix}. \quad (1)$$

without air-bridges can also be characterized simultaneously by taking parts of (2) into calculation

$$\begin{bmatrix} \boldsymbol{Y}_{xx}^{11} & \boldsymbol{Y}_{xy}^{11} \\ \boldsymbol{Y}_{yx}^{11} & \boldsymbol{Y}_{yy}^{11} \end{bmatrix} \begin{bmatrix} \boldsymbol{E}_x \\ \boldsymbol{E}_y \end{bmatrix} = \begin{bmatrix} \boldsymbol{J}_x \\ \boldsymbol{J}_y \end{bmatrix}. \tag{3}$$

Using the transmission line theory, we can easily extract scattering parameters for different modes from solutions of (2) and (3).

B. Experimental Consideration

The CPW mode is the one that can be launched and measured in our experimental setup. In addition to the CPW (even) mode, the asymmetrical discontinuity also excites the CSL (odd) mode. This excited CSL mode is assumed to be totally reflected back to the discontinuity by the SMA connector and generates the CSL-to-CPW mode conversion. Therefore, two independent excitations are needed to completely characterize the 2×2 scattering parameters of an asymmetrical circuit

$$\begin{bmatrix} b^e \\ b^o \end{bmatrix} = \begin{bmatrix} S_{11}^{ee} & S_{11}^{eo} \\ S_{11}^{oe} & S_{11}^{oo} \end{bmatrix} \begin{bmatrix} a^e \\ a^o \end{bmatrix}. \tag{4}$$

Here, for example, S_{11}^{ee} and S_{11}^{oe} are scattering parameters of reflected even and odd modes due to the even mode excitation. To make an approximation for the influence of the shorted CSL mode at the SMA connector, the modal amplitudes for the odd mode at the reference plane need to satisfy

$$a^o = -e^{-j\beta_o l} b^o; \qquad l = 2p + \Delta. \tag{5}$$

Here, p is the length of the uniform CPW section between the SMA connector and the reference plane. Δ denotes the equivalent length of the connector for the shorted odd mode. By a first-order approximation, the extension length includes a quarter of the circumference of the connector's outer conductor and an equivalent length of a shorted-end discontinuity [20]. Substituting (5) into (4), the measured scattering parameter can be related to the theoretical ones through

$$S_{11} = S_{11}^{ee} - \frac{S_{11}^{eo} S_{11}^{oe}}{e^{-j\beta_o l} + S_{11}^{oo}} \tag{6}$$

where $\beta_o l$ is the phase delay for the CSL wave scattered from and reflected back to the reference plane. For the symmetrical discontinuity, only the S_{11}^{ee} is calculated since the discontinuity does not excite the CSL mode for the CPW incident wave.

III. Results

A. CPW Discontinuities

The 3-D dyadic Green's function derived in Section II-A is for the NLC structure shown in Fig. 1. In our analysis, the Green's function for the CPW structure is obtained by choosing $\varepsilon_{r2} = 1$ and $h_2 = 50$ mm in (1). The Thru-Reflect-Line (TRL) calibration technique is performed on the HP 8510B Network Analyzer to accurately set the reference position and to eliminate the field mismatch at the SMA-to-CPW transition. For a symmetrical discontinuity, no air-bridges are needed in the simulation and measurement. Fig. 2 shows good agreement between simulated and measured data

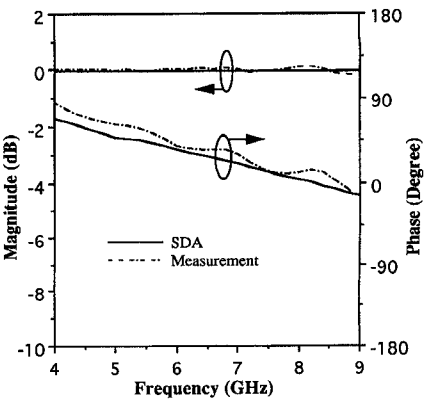

Fig. 2. Magnitude and phase of S_{11} of the symmetrical CPW discontinuity. Circuit dimensions: $\varepsilon_{r1} = 10.8, h_1 = 25$ mil, $w = 13.5$ mil, $s = 40$ mil, $a_r = a_l = 33.75$ mil, $b = 80$ mil.

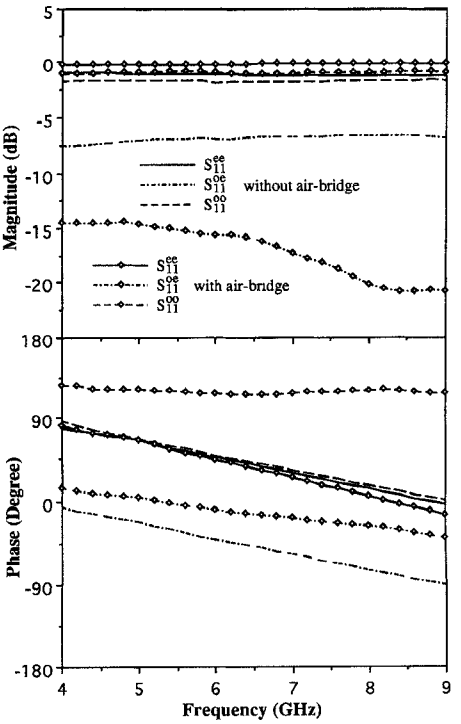

Fig. 3. Simulated scattering parameters of the asymmetrical CPW discontinuity without and with the air-bridge. Circuit dimensions are the same as those in Fig. 2 except that $a_r = 67.5$ mil, $a_l = 0, w_{ab} = 20$ mil, $d = 0.5 w_{ab}, y_{ab} = 0.1(s + 2w)$.

for a symmetrical discontinuity. The energy is completely reflected back from the discontinuity because the slotline is very short.

For the asymmetrical structure, we shift the slotline of the symmetrical one to the right hand side of the input CPW, i.e., $a_l = 0$ in Fig. 1. Fig. 3 shows the simulated amplitudes and phases of scattering parameters obtained from (2) and (3) for this asymmetrical discontinuity with and without the air-bridge, respectively. As one can see, the CPW-to-CSL mode conversion is about -7 dB without the air-bridge and it is reduced to almost less than -15 dB after adding the air-bridge. Also, power in CPW and CSL reflected waves increases with the existence of the air-bridge. The excited CSL mode is

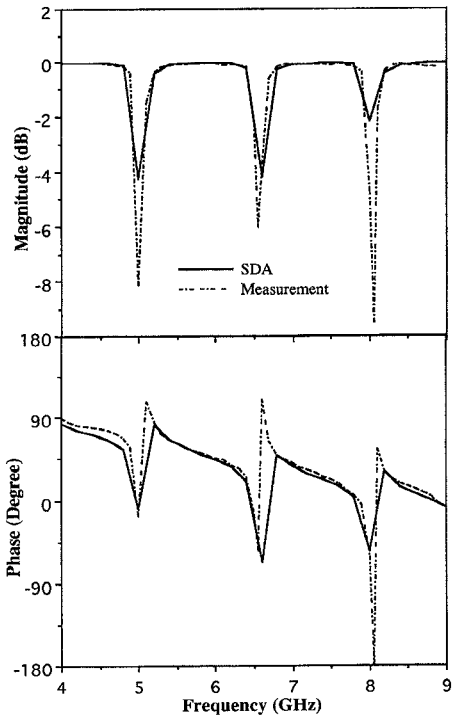

Fig. 4. Magnitude and phase of S_{11} of the CPW asymmetrical discontinuity without the air-bridge.

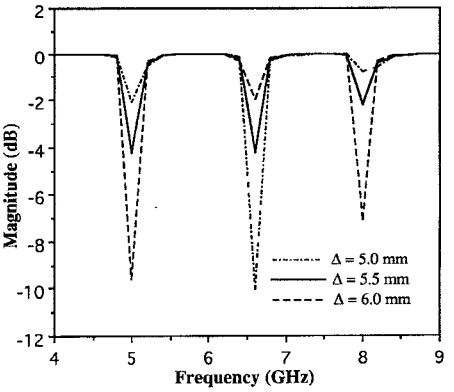

Fig. 5. Magnitude of S_{11} for different effective length Δ of the shorted CSL mode at the SMA connector.

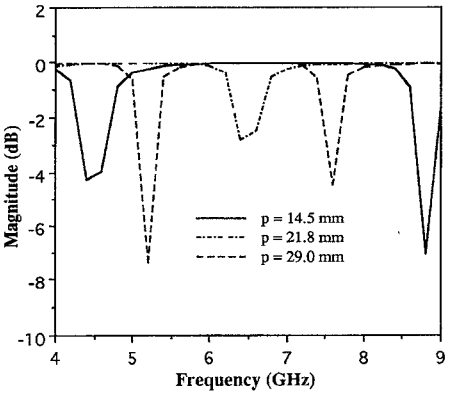

Fig. 6. Magnitude of S_{11} for different uniform CPW length p.

reflected back to the discontinuity if there are air-bridges at positions away from the discontinuity or the SMA connector in our experiment. Using (6), the simulated and measured S_{11}'s without air-bridges are shown in Fig. 4 where the uniform CPW length is: $p = 44.6$ mm and $\Delta = 5.5$ mm. Both amplitudes and phases agree very well. It can be seen that the reflected CSL mode affects the circuit without air-bridges drastically and creates some dips. The separation between dips is about a half-wavelength of the CSL mode. Hence, it is believed that a resonant circuit is formed for the CSL mode between the SMA connector and the end discontinuity at the frequency with a $|S_{11}|$ dip. The resonant CSL mode causes radiation loss and $|S_{11}|$ dips since the circuit is in an open space. One can conclude that the CSL mode plays a dangerous role if a single CPW mode propagation is needed. Since there is no rigorous prediction available for the value of Δ, the variation of S_{11} for different adjusted Δ's is shown in Fig. 5. The dip positions are properly predicted if Δ is in a reasonable range which is about a quarter of the circumference of the connector's outer conductor [20]. Nevertheless, the circuit performance is changed greatly as shown in Fig. 6 if the length p of the uniform CPW is altered markedly. In an uniplanar circuit module, mutiple circuit stages, e.g., multistage power amplifiers, are connected to each other by uniform CPW sections. Each stage may use several air-bridges to suppress the unwanted CSL mode. Therefore, air-bridges at adjacent stages and the length of the uniform CPW would affect the circuit performance if the excited CSL wave due to careless designs is large enough.

The simulated and measured S_{11}'s after adding the air-bridge is shown in Fig. 7. The dip phenomena are markedly reduced. The deviation of dip positions between simulated and measured data is caused mainly by the difference between the simulated model and the actually used air-bridge. There are still small dips on both curves, i.e., the used air-bridge could not eliminate the mode conversion completely. A small amount of the CSL mode still exists and affects the circuit performance. In order to obtain the optimal performance, the characteristic of the mode suppression by using air-bridges should be investigated completely. For example, Figs. 8–10 show the mode conversion versus the different air-bridge width, height, and position for two offset ratios of an offset-fed slot antenna. The offset ratio is defined as $(a_r - a_l)/(a_r + a_l)$. Although the excitation position is different, the trend of the CPW-to-CSL mode conversion is the same. It can be concluded that the suppression of the CSL mode by using an air-bridge for a CPW offset-fed slot antenna is more efficient for the air-bridge with the wider width, the lower height, and closer to the discontinuity.

B. NLC Waveguide Discontinuities

The analysis of the leakage control for NLC waveguide discontinuities is an important step to make this new guiding structure practical. The tested circuits are symmetrical and asymmetrical perturbations of the NLC shorted circuit. It will be discussed later that there is a power leakage caused by the SMA-to-NLC transition, and the circuit performance affected

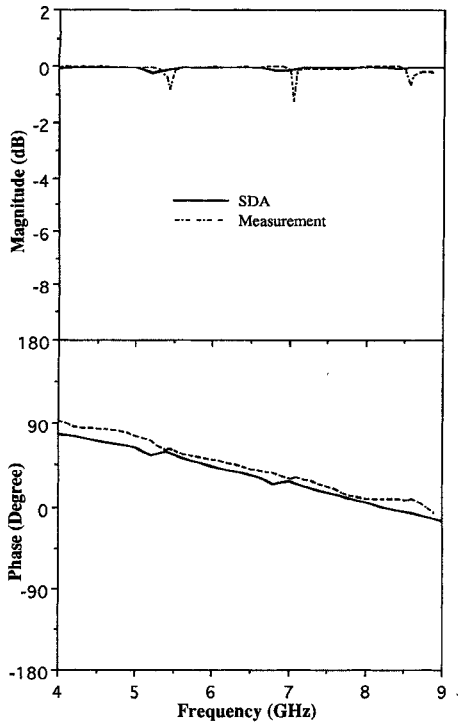

Fig. 7. Magnitude and phase of S_{11} of the asymmetrical CPW discontinuity with the air-bridge.

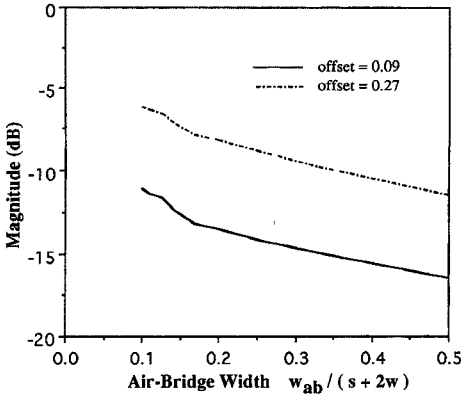

Fig. 8. CPW-to-CSL mode conversion $|S_{11}^{oe}|$ for the different air-bridge width.

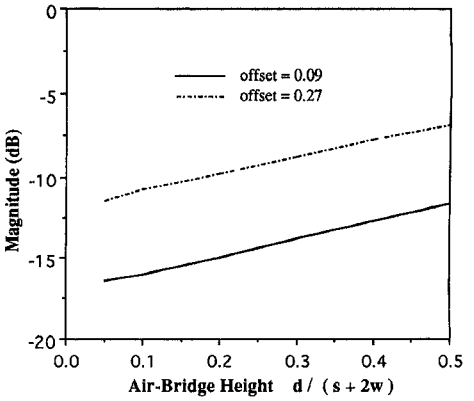

Fig. 9. CPW-to-CSL mode conversion $|S_{11}^{oe}|$ for the different air-bridge height.

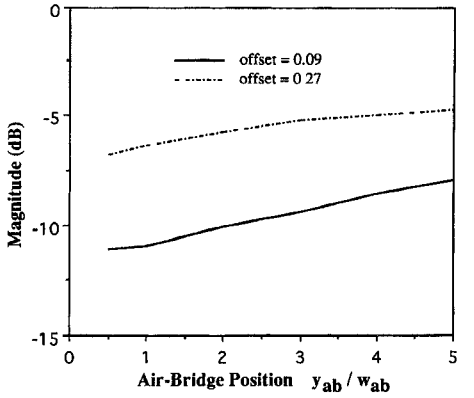

Fig. 10. CPW-to-CSL mode conversion $|S_{11}^{oe}|$ for the different air-bridge position.

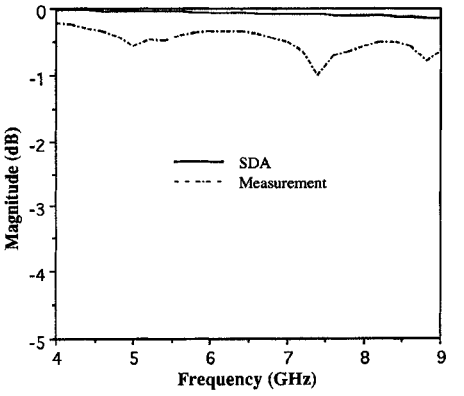

Fig. 11. Magnitude of S_{11} of the symmetrical NLC discontinuity. Circuit Dimensions: $\varepsilon_{r1} = 10.8, \varepsilon_{r2} = 2.2, h_1 = 50$ mil, $h_2 = 125$ mil, $w = 16$ mil, $s = 40$ mil, $a_r = a_l = 40$ mil, $b = 70$ mil.

by wave leakage depends on circuit dimensions. Therefore, the TRL calibration technique is not suitable for the present text fixture, because this technique requires three different sizes of NLC waveguides in our frequency range. The HP 8720A Network Analyzer with standard calibration kits is used in this subsection. Fig. 11 is the theoretical and measured scattering parameters of the symmetrical case. The trend for both curves is basically the same. The deviation of the power level is due to circuit loss and field mismatch at the launcher. From the theoretical result, this discontinuity does not seem to cause leakage. However, there are noticeable small ripples in the measured data. These ripples come from the leakage caused by discontinuities most likely the SMA-to-NLC transition. This point will be clear in subsequent experimental studies. Fig. 12 shows calculated and measured scattering parameters of the asymmetrical NLC discontinuity with an air-bridge. It is evident that S_{11}^{oe} is much smaller than that of S_{11}^{ee} and S_{11}^{oo}. Therefore the contribution of the second term in (6) is so small that the measured S_{11} is close to S_{11}^{ee}. There are still some ripples in the measured data of Fig. 12.

To see whether the measured ripples are caused by wave leakage, we measured these circuits with (marked as D) and without (marked as M) the surrounded absorbing material. Figs. 13 and 14 are measured results for symmetrical and

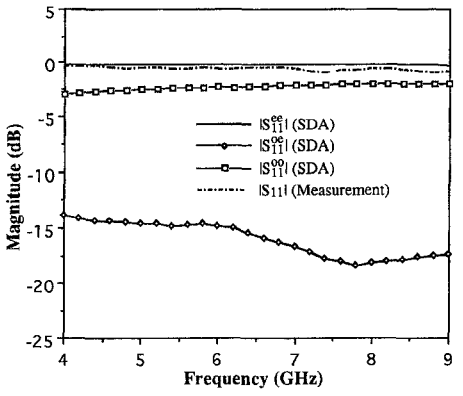

Fig. 12. Scattering parameters of the asymmetrical NLC discontinuity. Circuit dimensions are the same as those in Fig. 11 except that $a_r = 80$ mil, $a_l = 0, b = 70$ mil, $w_{ab} = 20$ mil, $d = 7$ mil, $y_{ab} = 10$ mil.

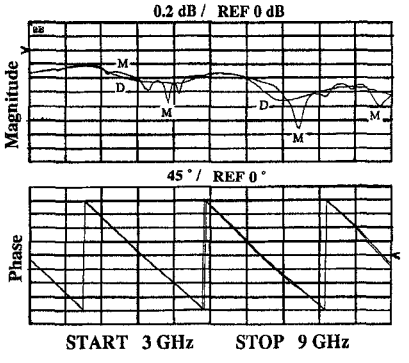

Fig. 13. Measured S_{11} with (D) and without (M) the surrounded absorbing material for the symmetrical NLC discontinuity.

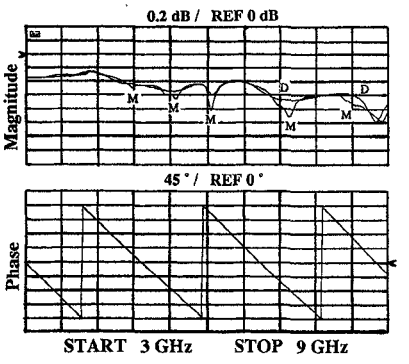

Fig. 14. Measured S_{11} with (D) and without (M) the surrounded absorbing material for the asymmetrical NLC discontinuity.

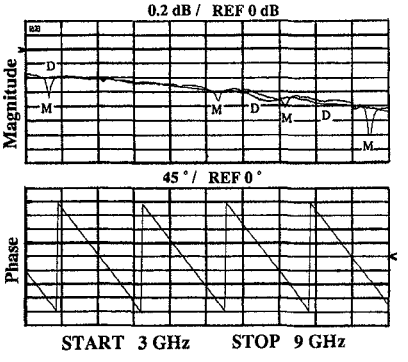

Fig. 15. Measured S_{21} with (D) and without (M) the surrounded absorbing material for the uniform NLC through-line.

asymmetrical cases, respectively. It is clear that the ripples are eliminated after the absorbing material is applied to take away the small power leakage. Since the leakage is small, the phase term does not change much for both situations. It is also observed that there are some common ripple positions for different measured circuits. Such ripples are considered to be caused by the same factor, i.e., the SMA-to-NLC transition. To verify this point, we measured the NLC through-line with and without the absorbing material. Fig. 15 shows that this transition does cause a power leakage. However, since Fig. 15 is for a two-port structure and the results depend on the line length, the locations of ripples in this figure are not related to those in Figs. 13 and 14. Unless this leakage from the launcher is eliminated, it is not possible to characterize NLC circuits exactly. Therefore, different launching techniques should be studied to prevent the power leakage.

C. Discussion

In comparison of Figs. 3 and 12, it is interesting to find that the CPW-to-CSL mode conversion with the air-bridge behaves almost the same for CPW and NLC waveguide with comparable metallization dimensions. During the experiment, there were small spikes (about 0.3 dB) in the TRL measurement of the LINE of calibration kits if the uniform 50 Ω CPW is soldered to the SMA connector directly. According to the analyses in Section III.A, it is believed that these spikes are caused mainly by the CSL and other higher order modes. These modes are easily excited due to circuit asymmetries and the strong field mismatch at the transition. Therefore, several SMA-to-CPW transitions are investigated to alleviate this problem. It is observed that the one with less field and impedance mismatch has almost invisible spikes (less than 0.1 dB). This optimal transition was applied to the measurement in Section III-A. Hence, a more careful design is needed for the transition if one uses the SMA connector as a launcher for CPW-like circuits. This is also why there are ripples in the experiment of NLC waveguides as the 50 Ω NLC waveguide is connected to the SMA connector directly. Consequently, other wave launching techniques, e.g., the probe excitation, for CPW-like structures are worth studying.

IV. Conclusion

The one-port symmetrical and asymmetrical discontinuities of coplanar and nonleaky coplanar waveguides are analyzed using the full-wave spectral domain analysis. The simulated data agree very well with those of measurement for CPW's with and without the air-bridge. The excited CSL mode due to circuit asymmetries drastically affects the circuit performance. It is observed that arbitrary air-bridge dimensions may not be sufficient to suppress the CSL mode to the level of not affecting the circuit. Therefore, the optimal air-bridge dimension for a specific circuit should be studied in advance. For a CPW offset-fed slot antenna, it is found that the

suppression is better by employing the wider, lower air-bridge which must also be close to the discontinuity.

Except for small ripples, theoretical and experimental data agree well for NLC waveguide discontinuities. These ripples represent the little amount of power leakage caused by the field mismatch and circuit discontinuities at the SMA-to-NLC transition. During the series studies of SMA-to-CPW transitions, it is believed that the leakage can be reduced with an appropriate transition design. Both field and impedance matches are critical if one uses the SMA connector to excite CPW-like structures. Other launching techniques are worth studying to prevent the power leakage.

ACKNOWLEDGMENT

The authors would like to thank Prof. R.-B. Wu of National Taiwan University for helpful discussions.

REFERENCES

[1] B. K. Kormanyos, W. Harokopus Jr., L. P. B. Katehi, and G. M. Rebeiz, "CPW-fed active slot antenna," *IEEE Trans. Microwave Theory Tech.*, vol. 42, pp. 541–545, Apr. 1994.

[2] N. H. L. Koster, S. Kosslowski, R. Bertengurg, S. Heinen, and I. Wolff, "Investigations on air bridges used for MMICs in CPW technique," in *Proc. 19th European Microwave Conf.*, pp. 666–671.

[3] M. E. Goldfarb and V. K. Tripathi, "The effect of air bridge height on the propagation characteristics of microstrip," *IEEE Microwave and Guided Lett.*, Oct. 1991, pp. 273–274.

[4] N. I. Dib, L. P. B. Katehi, and G. E. Ponchak, "Analysis of shielded CPW discontinuities with air-bridges," in *IEEE MTT-S Int. Microwave Symp. Dig.*, 1991, pp. 469–472.

[5] N. I. Dib and L. P. B. Katehi, "Characterization of non-symmetric coplanar waveguide discontinuities," *IEEE MTT-S Int. Microwave Symp. Dig.*, 1992, pp. 99–102.

[6] N. I. Dib, M. Gupta, G. Ponchak, and L. P. B. Katehi, "Characterization of asymmetric coplanar waveguide discontinuities," *IEEE Trans. Microwave Theory Tech.*, vol. 41, pp. 1549–1558, Sept. 1993.

[7] H. Jin and R. Vahldieck, "Calculation of frequency-dependent S-parameters of CPW air-bridges considering finite metallization thickness and conductivity," in *IEEE MTT-S Int. Microwave Symp. Dig.*, 1992, pp. 207–210.

[8] A. A. Omar and Y. L. Chow, "A solution of coplanar waveguide with air-bridges using complex images," *IEEE Trans. Microwave Theory Tech.*, vol. 40, pp. 2070–2077, Nov. 1992.

[9] T. Becks and I. Wolff, "Full-wave analysis of various coplanar bends and T-junctions with respect to different types of air-bridges," in *IEEE MTT-S Int. Microwave Symp. Dig.*, 1993, pp. 697–700.

[10] S. Visan, O. Picon, and V. F. Hanna, "3D characterization of air bridges and via holes in conductor-backed coplanar waveguides for MMIC applications," in *IEEE MTT-S Int. Microwave Symp. Dig.*, 1993, pp. 709–712.

[11] H. Shigesawa, M. Tsuji, and A. A. Oliner, "Conductor-backed slotline and coplanar waveguide: Dangers and full-wave analysis," in *IEEE MTT-S Int. Microwave Symp. Dig.*, 1988, pp. 199–202.

[12] Y. Liu and T. Itoh, "Control of leakage in multilayered conductor-backed coplanar structures," in *IEEE MTT-S Int. Microwave Symp. Dig.*, 1994, pp. 141–144.

[13] J.-W. Huang and C.-K. C. Tzuang, "Mode-coupling-avoidance of shielded conductor-backed coplanar waveguide (CBCPW) using dielectric lines compensation," *IEEE MTT-S Int. Microwave Symp. Dig.*, 1994, pp. 149–152.

[14] N. K. Das, "Two conductor-backed configurations of slotline or coplanar waveguide for elimination or suppression of the power-leakage problem," in *IEEE MTT-S Int. Microwave Symp. Dig.*, 1994, pp. 153–156.

[15] T. Becks and I. Wolff, "Analysis of 3-D metallization structures by a full-wave spectral domain technique," *IEEE Trans. Microwave Theory Tech.*, vol. 40, pp. 2219–2227, Dec. 1992.

[16] T.-S. Horng, "Extending the three-dimensional spectral-domain approach to hybrid microwave integrated circuits with passive and active lumped elements," in *IEEE MTT-S Int. Microwave Symp. Dig.*, 1994, pp. 709–712.

[17] ———, "A generalized method for evaluating the metallization thickness effects on microstrip structures," in *IEEE MTT-S Int. Microwave Symp. Dig.*, 1994, 1009–1012.

[18] M.-J. Tsai, T.-S. Horng, and N. G. Alexopoulos, " Via hole, bond wire and shorting pin modeling for multi-layered circuits," in *IEEE MTT-S Int. Microwave Symp. Dig.*, pp. 1777–1780.

[19] C.-Y. Lee and T. Itoh, "Full-wave analysis and design of a new double-sided branch-line coupler and its complementary structure," accepted for publication in *IEEE Trans. Microwave Theory Tech.*, vol. 43, Aug. 1995.

[20] M.-D. Wu, S.-M. Deng, R.-B. Wu, and P. Hsu, "Full-wave characterization of the mode conversion in a coplanar waveguide right-angled bend," submitted to *IEEE Trans. Microwave Theory Tech.*

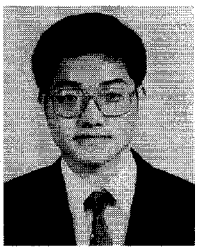

Chung-Yi Lee (S'94) was born in Hualien, Taiwan, on April 7, 1965. He received the B.S. degree from Chun Yuan Christian University, Chunli, Taiwan, the M.S. degree from the National Chiao Tung University, Hsinchu, Taiwan, and the Ph.D. degree from the University of California, Los Angeles, in 1987, 1989, and 1995, respectively.

From 1991 to 1992, he was on the faculty at the Chinese Junior College of Marine Technology, Taipei, Taiwan. From 1992 to 1995, he was a Graduate Student Researcher with the University of California, Los Angeles, where he is now a Postdoctoral Fellow. His research interests include wireless communications, microwave and millimeter-wave integrated circuits, antenna designs, and the development of electromagnetic simulation tools.

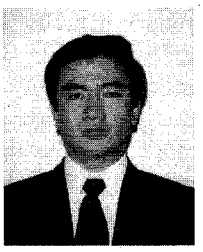

Yaozhong Liu (S'92) received the B.S. and M.S. degree from the Radio Electronics Department of Tsinghua University in 1983 and 1986, respectively. He is currently pursuing the Ph.D. degree at the University of California at Los Angeles (UCLA).

From 1986 to 1989, he worked in the Advanced Physics Laboratories at Tsinghua University in the area of superconductoring electronics. He has been a graduate student researcher since 1991 in the Department of Electrical Engineering at UCLA. His primary research work is in the field of various guided wave structures in the microwave and millimeter-wave circuits.

Tatsuo Itoh, for a photograph and biography, see p. 1874 of the August 1995 issue of this TRANSACTIONS.